MODELLING THERMODYNAMICS OF ALLOYS FOR FUSION APPLICATION -

A. Caro, P. Erhart, M. Serrano de Caro, B. Sadigh (Lawrence Livermore National Laboratory), S.G. Srinivasan, and C. Jiang (LANL). L. Malerba (Belgium), J. Wallenius (Sweden), A. Stukowski (Germany)

OBJECTIVE

This research has two main objectives:

- The development of computational tools to evaluate alloy properties, using the information contained in thermodynamic functions. We aim at improving the ability of classical potentials to account for complex alloy behavior; and,
- The application of these tools to predict properties of alloys under irradiation, in particular the FeCr system.

SUMMARY

We develop a strategy to model radiation damage in FeCr alloys, system in which magnetism introduces an anomaly in the heat of formation of the solid solution that is at the basis of its unique behavior. Magnetism has implications for the precipitation of excess Cr in the *a*' phase in the presence of heterogeneities. These complexities pose many challenges for atomistic (empirical) methods. To address such issues we develop a modified, many-body potential by rigorously fitting thermodynamic properties, including free-energy. Multi-million atom displacement Monte Carlo simulations in the transmutation ensemble, using both our new potential and our new MC code, are able to predict properties of non equilibrium processes like heterogeneous precipitation, and dislocation – precipitate interactions, enabling the study of hardening and embrittlement under irradiation.

Our work aims at developing theoretical and numerical methodologies that are directly applicable to multi-scale modeling addressing the specific issues related to multi-component, multi-phase systems in non-equilibrium states, such as solid-solution hardening, point defect-solute interactions, stoichiometry effects, static and dynamic strain aging, dislocation-solute interactions, and in general the aspects of microstructure evolution that are affected by irradiation. At its present stage of development, we have been able to predict numerous thermodynamic properties of FeCr mainly related to ordering and precipitation; we have found new intermetallic phases and suggested the existence of a dependence of the solubility limit on the degree of order of the alloy. At present, we are studying dislocation mobility in the solid solution and the heterogeneous phase, and we are developing a new algorithm to perform Monte Carlo simulations inside the miscibility gap, a technique that will allow us to study interfacial energies and nucleation sizes.

In collaboration with LANL, we have also studied the structural and elastic properties of cementite (Fe3C) from first principles calculations as a first step in the development of a classical potential for the Fe-C system able to describe the martensitic phase of steels. The paper is published.

In collaboration with European groups (Belgium, Sweden) we have performed a careful comparison between the two existing approaches to model FeCr at the level of interatomic

potentials, namely the European 2 band model and our composition dependent model. The paper is published.

In the algorithm development side, the work of B. Sadigh and P. Erhart on the mathematical formulation of a 'fluctuation constrained Metropolis Monte Carlo' has been finished, and with the visit of A. Stukowski from Germany it has just been implemented in Lammps, a free MD code from Sandia. He has also implemented our composition dependent model for molecular dynamics of FeCr into Lammps what makes it available for the community.

PROGRESS AND STATUS

In this report we will describe the work done to determine the influence of short range order (SRO) in the solubility of Cr in Fe, leaving a detailed description of the other subjects reported in the Summary in the corresponding publications.

SRO is an anomaly originated in the negative heat of formation (hof) of this alloy for Cr content below about 5 at%. In this region of composition, and because the negative hof, the mixture is expected to have ordered phases. In the period covered in the last report, we described our search for ordered intermetallic phases. Now we report on our findings regarding how short range order affects the location of the *solvus*, i. e. the solubility limit in FeCr.

By comparing the thermodynamics of the random alloy with the short-range ordered alloy, we extracted the contributions of SRO to the free energy coming from the enthalpy of mixing and from the vibrational and configurational entropies. We conclude that the effects of SRO are significant, doubling the solubility limit of Cr at low temperatures (≈300 K), and that this effect is mainly due to the contribution of SRO to the enthalpy.

We reassessed the previously published phase diagram [1, 2] by explicitly taking into account the effects of SRO on the three functions entering the expression for the free energy, namely, the mixing enthalpy and the vibrational and configurational entropies. We found significant effects of SRO on the location of the *solvus*. We also corrected an error in previous publications [1, 2] regarding the position of the miscibility gap according to the same cohesive model used here.

General methodology

Choice of cohesive model

The evaluation of thermodynamic functions requires information about the dynamical properties of the system, which usually are beyond the capabilities of *ab initio* techniques. Within the latter approach this difficulty is usually addressed by making use of approximations such as the harmonic assumption for vibrational entropies. Here, however, we follow a different strategy which first approximates the energy of the system in terms of a classical interatomic potential for the alloy, and from there the thermodynamic functions are obtained via computational thermodynamics. The interatomic potential for Fe–Cr used in this work, the so-called concentration dependent model (CDM), and the approach to

computational thermodynamics are described in detail in [3–8]. There are other cohesive energy models in the literature that, as this one, do not explicitly include magnetism but also reproduce well the Fe–Cr complex behavior. These are a cluster expansion (CE) developed by Lavrentiev *et al* [9] and a two-band model (2BM) interatomic potential developed by Olsson *et al* [10]. The CE involves a cohesive model that is only applicable on a rigid lattice, and thus inherently neglects the effects of relaxations and vibrations, so it is less suitable for the current study. The two interatomic potentials, 2BM and CDM, are ad hoc extensions of the embedded atom method (EAM) [11] where additional parameters describing the local concentration are introduced. Though both models are suitable for the current study, here we opted for the CDM whose predictions of ordering have recently been analyzed by Erhart *et al* [12] as part of the work funded by this program.

Free energy computation

In this work the free energy per particle $F(T)$ at a given temperature T is obtained through a thermodynamic integration between the state of interest and a reference state at temperature $T0$ of known free energy $F(T0)$ [13]. This methodology applied to solids is described by Frenkel and Ladd [31]. Its application to binary disordered solid solutions is explained and used in [4–8]. As a part of this work, modifications to the latter methodology are applied to account for SRO in binary solid solutions.

The configurational entropy per particle, $S\mathrm{conf}(x)$, is usually taken to be that of a perfectly random mixture, as we did in all our previous studies. However, the presence of SRO decreases the configurational entropy becoming one of the factors affecting the free energy that we address in this work.

To take into account the effects of order on the configurational entropy of the alloy, we worked out the connection between SRO and pair-probabilities and the relation between the latter and the entropy.

The methodology presented above has been implemented in a numerical package [4–8], the so-called thermodynamic package (TDP) that calculates the free energy for a certain atomic arrangement of atoms with a given degree of SRO, as a function of temperature.

Pair-probabilities and SRO

To quantify the SRO in the alloy, the Warren–Cowley parameter [14] was introduced as a tool to evaluate the pair-probabilities in an alloy. The SRO parameter, $\eta\nu\ \alpha$, in the νth nearest neighbor shell for a representative atom of type A in a binary AB alloy is defined. Combining the definition of the SRO parameter with the standard Ising theory for a binary alloy [15, 16], all the pair-probabilities are uniquely defined as a function of concentration and SRO parameter

This result is used below to estimate the configurational entropy For details see [G. Bonny, P. Erhart, A. Caro, R. C. Passianot, L. Malerba, and M. Caro. "The influence of short range order on the thermodynamics of Fe-Cr alloys. In press in Modelling and Simulations in Mat Sci and Eng. (2009)].

Implementation of SRO

Configurational entropy and SRO

The configurational entropy is a measure of the degree of disorder in an alloy. For a binary perfectly random alloy the configurational entropy assumes that all the lattice positions are equivalent and uncorrelated [19]. However, in an alloy with a certain degree of order not all lattice sites are equivalent and a certain degree of correlation exists between lattice positions. In the case of SRO, all lattice positions can be assumed to be equivalent and the correlation between lattice sites decreases fast with increasing distance. The cluster variation method (CVM) provides expressions for the entropy [15, 16, 17], which can take into account non-equivalent lattice sites and correlations up to a certain predefined basic cluster size. Each basic cluster is considered as an uncorrelated independent species, which means that all correlations are described within the basic cluster.

Since we aimed at describing states with a certain degree of SRO, we choose the basic clusters to be pairs. The CVM entropy including pairs up to the *n*th nearest neighbor distance in a bcc lattice is a known analytic function that reduces to the random entropy in the case of the randomly disordered alloy. Note that, for an alloy exhibiting SRO, lattice sites separated by long distances are uncorrelated. For the case under study, we verified that the inclusion of third nearest neighbour pairs modifies the entropy only by 0.005%, confirming the short range of the correlations.

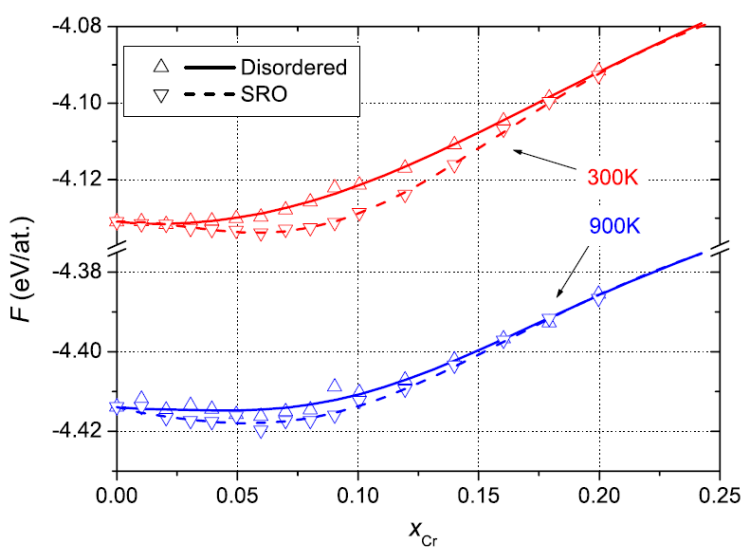

Figure 1: Isotherms of the free energy surface for the SRO and random alloy.

Post-processing

Following the procedure described in the previous section, a free energy surface for the disordered alloy and four free energy surfaces for the runs at 600–900K including a degree of order were obtained. To conveniently post-process the raw data, two Redlich–Kister (RK)-expansions [18] per data set were fitted, valid in the ranges 0–30%Cr and 30–100%, respectively.

The phase boundaries for the phase diagram are easily obtained from the parameterized free energy surfaces using the common tangent method [19]. Application of this method generated four sets of phase boundary curves, valid in the range around 300, 500, 700 and 900 K, for the SRO alloy. These four sets of boundaries are merged into one set of phase boundaries by means of a linear interpolation between two exact isotherms at *T*low and *T*high. Using this interpolation scheme, a phase diagram taking into account SRO is obtained that can be compared with the phase diagram corresponding to the randomly disordered alloy.

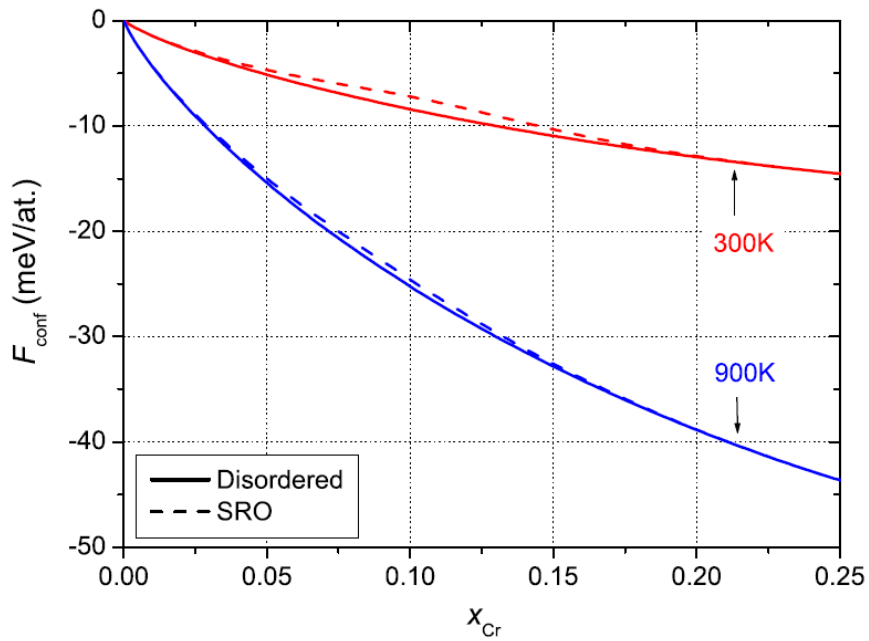

Figure 2: Isotherms of the configurational free energy for the SRO and random alloy.

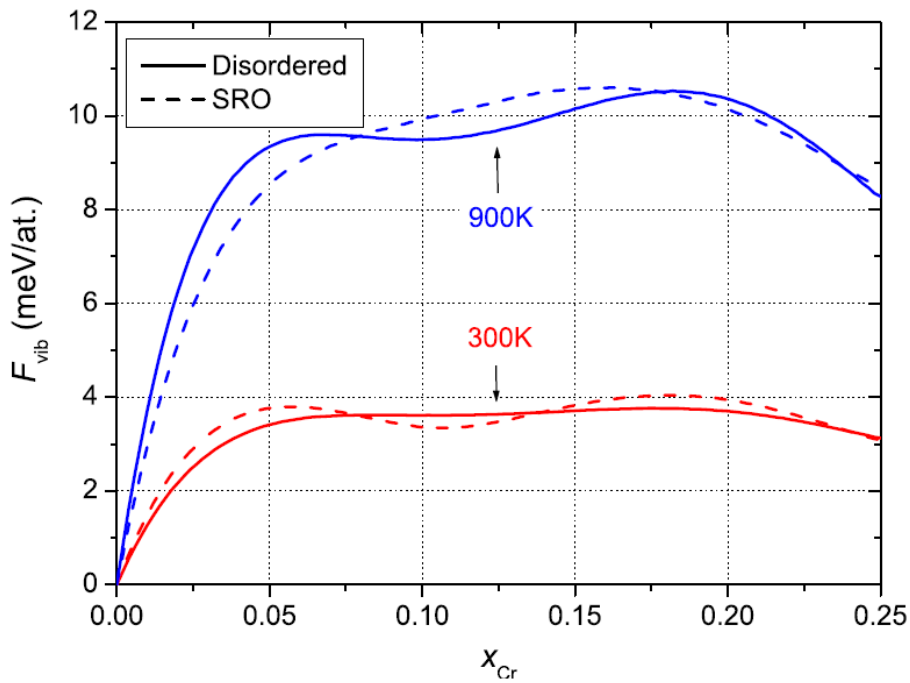

Figure 3: Isotherms of the excess vibrational free energy for the SRO and random alloy.

Thermodynamic functions

Two isotherms at 300 and 900K are shown in figure 1. In this plot the free energy from the random and SRO alloys are compared. To illustrate the quality of the RK-expansion fit, the raw data are superposed on the fits, represented by the full lines. From the plot it is clear that the isotherms for the SRO alloy are lower than the isotherms of the random alloy. The difference is about 7 meV atom−1 at 300K and 4 meV atom−1 at 900 K. To investigate the origin of this difference, the free energy is further separated in the enthalpy and entropy contributions, as described in appendix A and discussed below.

The contribution of the configurational entropy to the free energy, Fconf = $-T$ Sconf, is presented in figure 2 where the configurational free energy for the random and SRO alloy are compared at 300 and 900 K. As expected, SRO pushes the configurational free energy up. The magnitude by which the free energy is shifted, however, is less than 1.3 meV atom−1 at 300K and 0.7 meV atom−1 at 900 K, which is of the order of magnitude of the numerical errors. We conclude then that the effect of SRO on the configurational entropy is of minor importance; therefore the past/future use of the disordered configurational entropy is justified, a statement that represents a first conclusion of this work.

The effect of the SRO on the excess vibrational free energy, Fvib = $-T$ Svib, is illustrated in figure 3 for the temperatures 300 and 900 K. Here too the difference between the SRO and random solutions is less than 1 meV, which makes us conclude that the effect of SRO on the vibrational entropy is negligible. It should be noted, however, that in this concentration range the excess vibrational free energy is positive and acts opposite to the configurational free

energy, but is about four times smaller in absolute value, i.e. has a negligible contribution to the stability of the phase. This result is in agreement with direct vibrational entropy calculations using the same potential performed in [20, 21]. It is however contrary to experimental observations, where the excess vibrational free energy is found to be negative and not negligible by −0.18 and −0.20kB atom−1 for a random Fe53Cr47 alloy at 300K and the high temperature limit [22], respectively. However, this shortcoming of the potential is not expected to affect the outcome of this study at a low temperature, even compared with experiments.

The effect of the SRO on the excess enthalpy is illustrated in figure 4 at the temperatures 300 and 900 K. It is clear that the difference between the SRO and random solutions is significant, about 8 meV at 300K and 4 meV at 900 K. Note that the excess enthalpy is independent of temperature for the random case, while it is strongly temperature dependent in the SRO case. This is due to the changes in SRO of the alloy with temperature, as shown.

Thus the combined effect of the SRO on the configurational entropy, the excess vibrational entropy and the excess enthalpy gives a significant shift in the free energy. From this discussion it is clear that this effect is dominated by the enthalpy, thereby stressing the importance of having the latter quantity properly described by the cohesive model.

The phase diagram

The shift in free energy introduced by SRO is translated into a shift of the Fe-rich phase boundary presented in figure 5. The phase boundary is shifted towards the Cr-rich side by approximately 4% Cr at a low temperature, an amount that implies doubling the solubility limit of Cr in the α phase. This shift, however, decreases fast with increasing temperature and disappears at about 900 K, even though SRO is still present. This observation suggests that the sudden disappearance of SRO due to the magnetic transition from ferro to para-magnetism (at Curie temperature, TCurie ≈ 1050 K) will not have a drastic impact on the phase diagram. Therefore the phase boundary is expected to show a smooth transition at the Curie temperature. At the Cr-rich side the phase boundary remains unchanged, as expected, since the Cr-rich alloy does not exhibit SRO.

In figure 6 our prediction for the Fe-rich phase boundary is compared with the standard CALPHAD phase diagram (in the range of the ferro-magnetic phase outside the range of formation of the σ-phase) [23, 24] and with some experimental low temperature data points from the works of Filippova *et al* [25] and Kuwano [26], which include data from both irradiation and thermal ageing experiments, respectively. In both works Moessbauer spectroscopy was used to identify SRO or α' precipitation. In the plot, the square (green) points denote the observed SRO, the bold (black) points denote precipitates observed and the italic (red) points denote estimated phase boundary points by the respective authors. The low temperature data come from irradiated samples. Taking this into account, the experimental data points are used to describe the low temperature phase diagram, other than CALPHAD, which does not take low temperature data into account. Furthermore, the low temperature CALPHAD phase boundary is not consistent with the experimentally observed SRO at low Cr content.

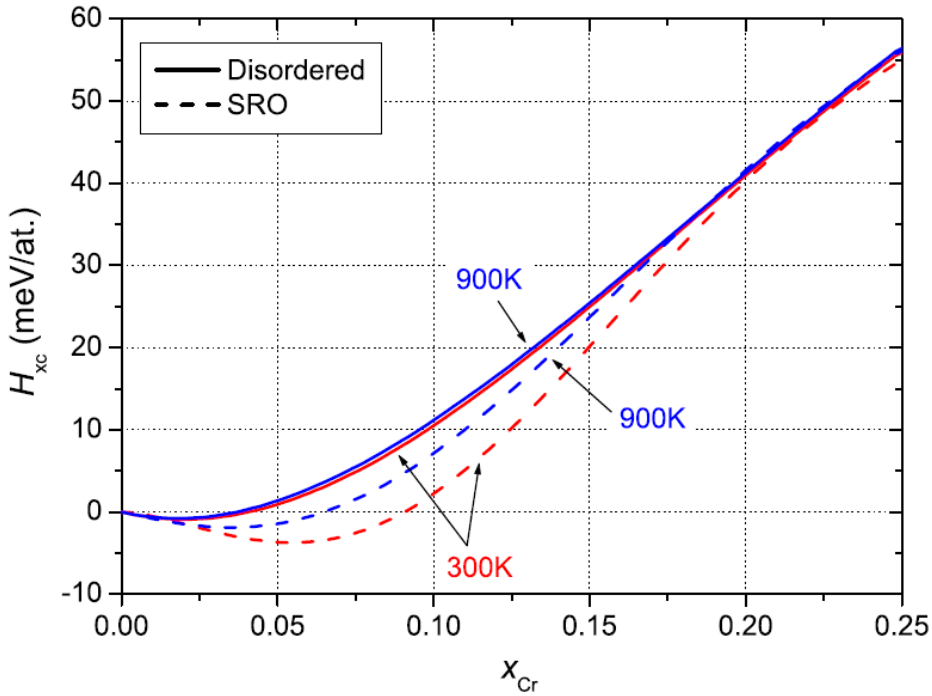

Figure 4: Isotherms of the excess enthalpy for the SRO and random alloy.

Figure 6 shows that the phase boundary obtained from our simulations matches the experimental data quite closely at temperatures below 700 K, with the salient feature that the *solvus* is very steep, and the Cr solubility at low *T* is very large, in contrast to the commonly accepted phase diagram of Fe–Cr. At higher *T*'s the discrepancy is significant as the miscibility gap does not close under melting temperature ≈2000 K, whereas the ferromagnetic metastable (neglecting the slow σ formation) miscibility gap closes around 900K [16]. This only reflects that the cohesive model and its predictions are valid at T's low compared with the FM/PM transition. [20, 21].

Conclusions

We have then investigated the effect of SRO on the thermodynamic properties of the Fe–Cr alloys by means of atomistic simulations. The free energy of the SRO alloy is significantly lower than the random alloy at low temperature and still noticeably lower at high temperature: the decrease in free energy due to SRO is attributed mainly to the decrease in enthalpy. The difference in the configurational and vibrational entropy between the SRO and random alloy is significantly smaller than in the case of the enthalpy. In fact, the effect of the configurational and vibrational entropy falls within the numerical precision of the calculations and is therefore of minor importance. Improvements in the description of the excess vibrational entropy may slightly affect these results but not invalidate the general conclusion that indicates that the *solvus* is quite steep and that the solubility of Cr is further enhanced by the development of order in the alloy.

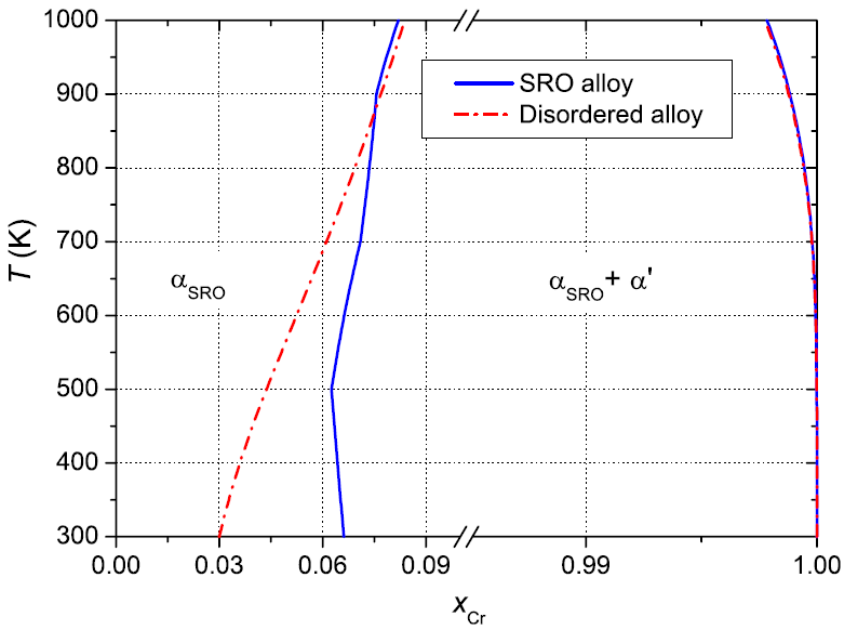

Figure 5: The phase boundaries for the SRO and random alloy.

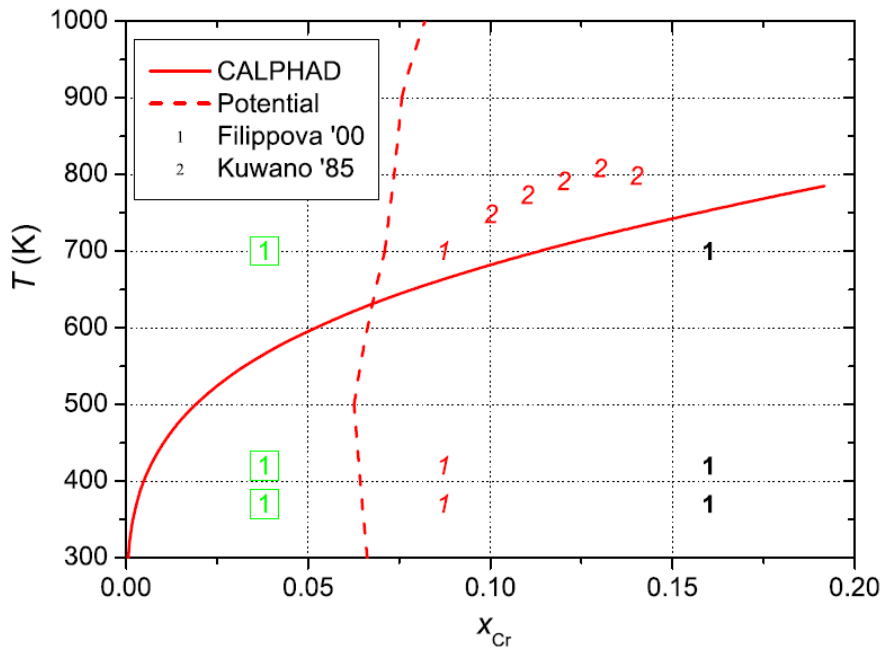

Figure 6: The phase diagram obtained from our simulations compared with experimental data. The points outlined in boxes (green in the online version) denote the observation of SRO, the points in bold font (black in the online version) denote precipitation observed, and the points in italic font (red in the online version) denote estimated phase boundary points by the respective authors.

The effect of SRO on the Fe-rich phase boundary is significant at a low temperature, where the boundary is shifted towards the Cr-rich region by almost doubling the solubility limit compared with the phase boundary for the random alloy. At about 900K the phase boundaries obtained from the SRO alloy and the random alloy coincide, while SRO is still observed in agreement with experiments where SRO is expected up to the Curie temperature [27]. This suggests only a minor impact of disordering due to the magnetic transition at the Curie temperature on the phase boundaries.

In summary, the main contributions of this work are as follows.

• The implications of the change in sign in the heat of mixing of Fe–Cr at a low Cr composition imply dramatic changes in the phase diagram, showing large solubility at low *T* and a steep phase boundary.

• A consequence of the complex heat of mixing and tendency to order is that the calculation of the thermodynamic functions must include the presence of SRO, whose influence on the location of the *solvus* is significant.

• The results presented in this work, based on *ab initio* energetics and interatomic potentials thermodynamics, seem to match well the experimental phase diagram below 700K and is in striking contrast to the phase diagram of Fe–Cr as appears in the CALPHAD database.

References

[1] Caro A, Caro M, Lopasso E M and Crowson D A 2006 *Appl. Phys. Lett.* **89** 121902

[2] Caro A, Caro M, Klaver P, Sadigh B, Lopasso E M and Srinivasan S G 2007 *TMS JOM* **59** 50

[3] Caro A, Crowson D A and Caro M 2005 *Phys. Rev. Lett.* **95** 75702

[4] Ogando Arregui E, Caro M and Caro A 2002 *Phys. Rev.* B **66** 054201

[5] Ogando E, Caro M and Caro A 2002 *Comput. Mater. Sci.* **25** 297

[6] Lopasso E M, Caro M, Caro A and Turchi P E A 2003 *Phys. Rev.* B **68** 214205

[7] Caro A, Turchi P E A, Caro M and Lopasso E M 2005 *J. Nucl. Mater.* **336** 233

[8] Caro A, Caro M, Lopasso E M, Turchi P E A and Farkas D 2006 *J. Nucl. Mater.* **349** 317

[9] Lavrentiev M Y, Drautz R, Nguyen-Manh D, Klaver T P C and Dudarev S L 2007 *Phys. Rev.* B **75** 14208

[10] Olsson P, Wallenius J, Domain C, Nordlund K and Malerba L 2005 *Phys. Rev.* B **72** 214119

[11] Daw M S and Baskes M I 1984 *Phys. Rev.* B **29** 6443

[12] Erhart P, Caro A, Serrano de Caro M and Sadigh B 2008 *Phys. Rev.* B **77** 134206

[13] Frenkel D and Smit B 1996 *Understanding Molecular Simulation—From Algorithms to Applications* [14] Cowley J M 1950 *Phys. Rev.* **77** 669

[15] Inden G and Pitsch W 1991 *Materials Science and Technology* (*Phase Transformations in Materials* vol 5). Ed R W Cahn *et al* (Weinheim: Wiley) p 497

[16] Ducastelle F 1991 *Cohesion and structure* (*Order and phase stability in alloys* vol 3) (Amsterdam: North-Holland)

[17] Kikuchi R 1951 *Phys. Rev.* **81** 988

[18] Redlich O and Kister A T 1948 *Indust. Eng. Chem.* **40** 345

[19] DeHoff R T 2006 *Thermodynamics in Materials Science* (London: CRC Press)

[20] Pasianot R C, Bonny G and Malerba L 2007 *Proc. Congreso SAM/CONAMET (San Nicolas)*

[21] Bonny G, Pasianot R C, Malerba L, Caro A, Olsson P and Lavrentiev M Yu 2008 Numerical prediction of thermodynamic properties of Fe–Cr alloys using semi-empirical cohesive models: where do westand? *J. Nucl.Mater.* submitted

[22] Fultz B, Anthony L, Robertson J L, Nicklow R M, Spooner S and Mostoller M 1995 *Phys. Rev.* B **52** 3280

[23] Andersson J-O and Sundman B 1987 *CALPHAD* **11** 83

[24] Saunders N and Miodownik A P 1998 *CALPHAD (Calculation of Phase Diagrams): A Comprehensive Guide* (*Pergamon Materials Series* vol 1) ed R W Cahn (Oxford: Pergamon)
[25] Filippova N P, Shabashov V A and Nikolaev A L 2000 *Phys. Met. Metallogr.* **90** 145 AQ6
[26] Kuwano H 1985 *Trans. Japan Inst. Met.* **26** 473
[27] Mirebeau I, Hennion M and Parette G 1984 *Phys. Rev. Lett.* **53** 687
(London: Academic Press)